



Available online at <http://scik.org>

Commun. Math. Biol. Neurosci. 2025, 2025:12

<https://doi.org/10.28919/cmbn/9036>

ISSN: 2052-2541

TRANSMISSION DYNAMICS OF YELLOW FEVER WITH TOXIC INFECTED POPULATION

ELVIS KOBINA DONKOH¹, BAABA ABASSAWAH DANQUAH¹, FRANÇOIS MAHAMA³,
DAUDA MUSAH¹, FRANCIS TUFFOUR¹, KENNEDY MENSAH^{1,2}, KWAME KYEI DANQUAH⁴

¹Department of Mathematics and Statistics, University of Energy and Natural Resources, Sunyani, Ghana

²Department of Mathematics, Kwame Nkrumah University of Science and Technology, Kumasi, Ghana

³Department of Mathematics and Statistics, Ho Technical University, Ho, Ghana

⁴Department of Mathematics, Ghana Secondary Technical School, Takoradi, Ghana

Copyright © 2025 the author(s). This is an open access article distributed under the Creative Commons Attribution License, which permits unrestricted use, distribution, and reproduction in any medium, provided the original work is properly cited.

Abstract. Yellow fever is currently affecting the African subcontinent, with Ghana accounting for the majority of confirmed cases (37.7%). As infections resurface in regions that have been free of yellow fever for more than a decade, it has become crucial to develop a mathematical model that accurately represents the transmission dynamics of yellow fever within a toxic infected population. The analysis of the existence and stability of the models' equilibrium points is conducted. The sensitivity index study revealed that \mathbf{a} , β_1 , β_2 , Λ , γ were the most sensitive parameters influencing the spread of yellow fever. The model is numerically solved using MATLAB ODE45 to determine its epidemiological implications. Preventing the advancement from infected (I_H) to toxic infected (D_H) individuals is essential, necessitating prompt intervention; hence, to mitigate the spread, it is imperative to decrease the contact rate between D_H and the susceptible individuals. The dynamics of D_H emphasize the significance of focusing on severe cases, for controlling outbreaks. Also, the stabilization phase of infected vectors suggests that measures aimed at vector reproduction or mortality may help limit the spread over time.

Keywords: yellow fever; basic reproductive number; local and global stability; sensitivity analysis; trivial equilibrium.

2020 AMS Subject Classification: 34D23, 34A34, 37N25.

*Corresponding author

E-mail address: kmensah33@st.knust.edu.gh

Received November 26, 2024

1. INTRODUCTION

Yellow fever(YF)is an infectious disease that is persistent in Africa [1]. It is a viral disease and one of the most dangerous diseases spread by mosquitoes. It is transmitted to humans through the bite of infected mosquitos, specifically the Aedes and Haemagogus mosquito species. It is an overlooked tropical infection that has received limited research attention [2]. YF is predominantly found in Africa, Central and South America, but it has previously caused huge epidemics in Europe and North America [3].

Recent outbreaks in Angola (2015-2016) [4] and Brazil (2016-2017) [5] highlight the virus's continued threat to public health. Yellow fever cases have risen dramatically over the last 15 years, with the majority occurring in West Africa [6].

The incidents persist in Africa and South America. Predicting the epidemics requires considering local mosquito populations, YF virus strain, eco-climatic conditions, sociopolitical and demographic factors, and vaccine coverage [7]. YF remains a significant hazard to public health, particularly in Africa, where it infects an estimated 840,000-1.7 million people annually, causing 84,000-170,000 severe cases and 29,000-60,000 fatalities [8]. Ghana recently experienced a YF outbreak in the Savannah region, resulting in 70 confirmed cases and 30 deaths [9].

Mathematical modeling has significantly enhanced the potential for intervening in vector-borne neglected tropical diseases. Recent epidemiological research has demonstrated the importance of mathematical modeling in combating infectious disease outbreaks [6].

[6] proposed a mathematical model to analyze the transmission patterns of YF, considering human and vector (mosquito) populations. Their model was solved numerically using the 4th-order Runge-Kunta scheme and their results demonstrate that control strategies such as reducing mosquito biting rates, human-vector transmission rates, and raising vaccine success rates can successfully slow disease spread.

[3] developed a sophisticated mathematical model to examine and simulate crucial epidemiological mechanisms behind the Angola YF outbreak. Their model was calibrated to measure YF cases and fatalities, while the basic reproduction number (R_0) was determined as a measure of time. Although their research sheds light on the dynamics of YF breakout in Angola, but

did not establish a theoretical stability for the disease to die out. [10] presented a fractional YF virus model, incorporating the Caputo derivative to analyze the dynamics of yellow fever virus transmission. Their results show that the Caputo fractional derivative provides more realistic information than the classical derivative and that the Adams-Bashfort-Moulton predictor-corrector method gives the expected depiction of the results for analyzing the dynamics of the projected model.

According to [11], YF is plaguing the African subcontinent, and according to Eliminate YF Epidemics (EYE), more than 25 African countries are classified as high-risk countries. Although the EYE strategy is a global plan to eradicate YF outbreaks by 2026, Ghana has been reported to have the majority of the confirmed cases (37.7%) [12]. As infections reoccur in regions that have been free of YF for over 10 years, it has become essential to develop a mathematical model that captures the transmission dynamics of yellow fever within a toxic infected population.

2. MODEL FORMULATION AND DESCRIPTION

A mathematical model for the transmission dynamics of YF within human and vector (mosquito) population is proposed. The human (N_H) and vector (N_V) populations are considered to be divided into compartments represented by state variables that change over time. N_H comprises of Susceptible S_H , Exposed E_H , Infected I_H , Toxic infected D_H , Vaccinated V_H , and Recovered R_H humans. Similarly, N_V includes Susceptible S_V , Exposed E_V , and Infected I_V mosquitoes. Hence, the total population is denoted as

$$(1) \quad N(t) = S_H + E_H + I_H + D_H + V_H + R_H + S_V + E_V + I_V$$

Figure 1 presents the transfer diagram of transmission dynamics of yellow fever within two different populations.

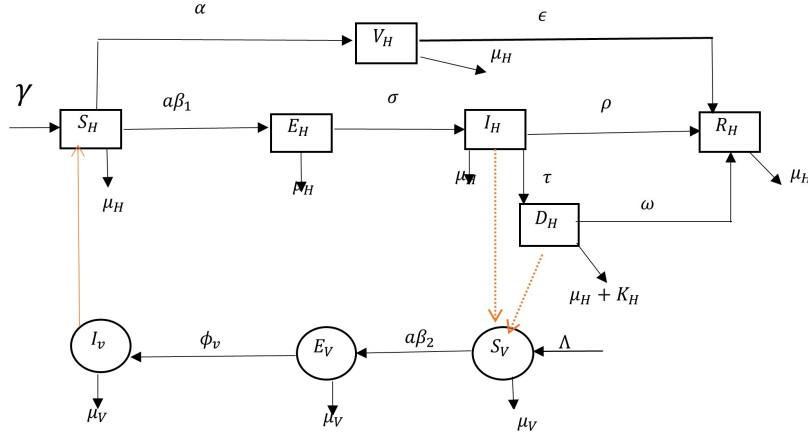


FIGURE 1. Model formulation for YF.

Thus the model equations given the transfer diagram 1:

$$(2) \quad \left\{ \begin{array}{l} \frac{dS_H}{dt} = \gamma - \lambda_1 S_H - \mu_H S_H - \alpha S_H \\ \frac{dE_H}{dt} = \lambda_1 S_H - (\sigma + \mu_H) E_H \\ \frac{dI_H}{dt} = \sigma E_H - (\mu_H + \rho + \tau) I_H \\ \frac{dD_H}{dt} = \tau I_H - (\mu_H + K_H + \omega) D_H \\ \frac{dV_H}{dt} = \alpha S_H - \epsilon V_H - \mu_H V_H \\ \frac{dR_H}{dt} = \omega D_H + \rho I_H + \epsilon V_H - \mu_H R_H \\ \frac{dS_V}{dt} = \Lambda - \lambda_2 S_V - \mu_V S_V \\ \frac{dE_V}{dt} = \lambda_2 S_V - (\phi_V + \mu_V) E_V \\ \frac{dI_V}{dt} = \phi_V E_V - \mu_V I_V \end{array} \right.$$

with initial conditions $S_H = S_H(0), E_H = E_H(0), I_H = I_H(0), D_H = D_H(0), V_H = V_H(0), R_H = R_H(0), S_V = S_V(0), E_V = E_V(0), I_V = I_V(0)$, where λ_1 and λ_2 are defined as $\lambda_1 = a\beta_1 I_V$ and $\lambda_2 = a\beta_2 (I_H + D_H)$.

TABLE 1. The description of the state variables of the YF model.

Variable	Description
S_H	number of Susceptible individuals
E_H	number of Exposed individuals
I_H	number of Infected individuals
D_H	number of Toxic infected individuals
V_H	number of Vaccinated individuals
R_H	number of Recovered individuals
S_V	number of Susceptible vectors
E_V	number of Exposed vectors
I_V	number of Infected vectors

Theorem 1. *Positivity and boundedness of solutions*

Given $\{S_H(t), E_H(t), I_H(t), D_H(t), V_H(t), R_H(t), S_V(t), E_V(t), I_V(t)\} \geq 0$ of system (2), then the set $\{S_H(t), E_H(t), I_H(t), D_H(t), V_H(t), R_H(t), S_V(t), E_V(t), I_V(t)\}$ of solutions are non-negative and bounded $\forall t > 0$ if there exist $\limsup_{t \rightarrow \infty} N_H(t) \leq \frac{\gamma}{\mu_H + \alpha}$, and $\limsup_{t \rightarrow \infty} N_V(t) \leq \frac{\Lambda}{\mu_V}$.

Proof. Suppose $t_1 = \sup\{t > 0 : S_H(t), E_H(t), I_H(t), D_H(t), V_H(t), R_H(t), S_V(t), E_V(t), I_V(t)\} \geq 0$. It is sufficient for $t_1 > 0$, since all the compartments are more than zero.

If $t < \infty$ then the state variables are equal to zero. From the susceptible individuals compartment of system (2),

$$\begin{aligned} \frac{dS_H}{dt} &= \gamma - \lambda_1 S_H - \mu_H S_H - \alpha S_H \\ \frac{dS_H}{dt} + (a\beta_1 I_V + \mu_H + \alpha) S_H &= \gamma \\ \frac{d}{dt} \left\{ S_H e^{(a\beta_1 I_V + \mu_H + \alpha)t} \right\} &= \gamma e^{(a\beta_1 I_V + \mu_H + \alpha)t} \\ S_H(t_1) e^{(a\beta_1 I_V + \mu_H + \alpha)t_1} - S_H(0) &= \int_0^{t_1} \gamma e^{(a\beta_1 I_V + \mu_H + \alpha)t} dt > 0 \end{aligned}$$

$$S_H(t_1) = S_H(0) e^{-(a\beta_1 I_V + \mu_H + \alpha)t_1} + e^{-(a\beta_1 I_V + \mu_H + \alpha)t_1} \int_0^{t_1} \gamma e^{(a\beta_1 I_V + \mu_H + \alpha)t} dt > 0.$$

Thus $S_H(t_1) > 0$. A similar approach on the rest of the compartments shows a positive states whenever $t > 0$.

Now, for boundedness,

$$0 < I_H < N_H \quad \text{and} \quad 0 < I_V < N_V$$

Adding the human compartments of model (2) gives:

$$\begin{aligned} \frac{dN_H}{dt} &= \gamma - N_H\mu_H - D_H K_H \\ \gamma - (\mu_H - D_H K_H)N_H &\leq \frac{dN_H}{dt} \leq \gamma - N_H\mu_H \\ \frac{\gamma}{\mu_H + D_H K_H} &\leq \liminf_{t \rightarrow \infty} N_H(t) \leq \limsup_{t \rightarrow \infty} N_H(t) \leq \frac{\gamma}{\mu_H + \alpha} \end{aligned}$$

Similarly, for the vector population:

$$\begin{aligned} \frac{dN_V}{dt} &= \Lambda - \mu_V N_V \\ \Lambda - \mu_V N_V &\leq \frac{dN_V}{dt} \leq \Lambda - \mu_V N_V \\ \frac{\Lambda}{\mu_V} &\leq \liminf_{t \rightarrow \infty} N_V(t) \leq \limsup_{t \rightarrow \infty} N_V(t) \leq \frac{\Lambda}{\mu_V} \end{aligned}$$

Hence, the state variables are bounded. □

3. MODEL ANALYSIS

3.1. Disease Free Equilibrium (\mathfrak{E}_0).

The YF model (2) has a point \mathfrak{E}_0 , obtained by setting the right-hand sides of the equations and the infected classes ($E_H, I_H, D_H, V_H, R_H, S_V, E_V, I_V$) to zero.

$$\mathfrak{E}_0 = \left(\frac{\gamma}{\mu_H + \alpha}, 0, 0, 0, \frac{\alpha\gamma}{(\mu_H + \alpha)(\varepsilon + \mu_H)}, 0, \frac{\Lambda}{\mu_V}, 0, 0 \right)$$

TABLE 2. Biological parameters and their descriptions along with values and references.

Parameter	Description	Value	Reference
a	Mosquito daily biting rate	0.5-0.7	[13]
β_1	Transmission probability from vector to host	0.3 per bite	[14]
σ	Progression rate from exposed to infected class in human	3-6 days	[3]
γ	Recruitment rate of human	10-800 per day	[15]
μ_H	Natural death rate for human	4.94×10^{-5}	[16]
μ_V	Natural death rate for vector	0.35	[16]
Λ	Recruitment rate of mosquito	0.051	[15]
α	Effective vaccination rate of susceptible human	0.043 per day	[3]
β_2	Transmission probability from host to vector	0.6 per bite	[17]
ε	Progression rate from vaccinated to recovered class	0.143 day^{-1}	[17]
ρ	Progression rate from infected to recovered class	0.143 day^{-1}	[3]
K_H	Disease-induced death rate	$3.5 \times 10^{-4} \text{ day}^{-1}$	[3]
τ	Progression rate from infected to toxic infected class	15%	[3]
ϕ_V	Progression rate from exposed to infected class in vector	1/18	[3, 6]
ω	Progression rate from toxic infected to recovered class	0.143 day^{-1}	[3, 18]

3.2. The basic reproductive number (\mathfrak{R}_0).

Using the Next Generation Matrix approach, matrices F and V are key components used to calculate \mathfrak{R}_0 and analyze the stability of disease-free equilibria [19].

$$F = \begin{pmatrix} a\beta_1 S_H I_V \\ 0 \\ 0 \\ a\beta_2 S_V (I_H + D_H) \\ 0 \end{pmatrix}, \text{ and } V = \begin{pmatrix} (\sigma + \mu_H) E_H \\ -\sigma E_H + (\mu_H + \rho + \tau) I_H \\ -\tau I_H + (\mu_H + K_H + \omega) D_H \\ (\phi_V + \mu_V) E_V \\ -\phi_V E_V + \mu_V I_V \end{pmatrix}.$$

$$J_F = \begin{pmatrix} 0 & 0 & 0 & 0 & \frac{a\beta_1 \gamma}{\mu_H + \alpha} \\ 0 & 0 & 0 & 0 & 0 \\ 0 & 0 & 0 & 0 & 0 \\ 0 & \frac{a\beta_2 \Lambda}{\mu_V} & \frac{a\beta_2 \Lambda}{\mu_V} & 0 & 0 \\ 0 & 0 & 0 & 0 & 0 \end{pmatrix}$$

$$J_V = \begin{pmatrix} (\sigma + \mu_H) & 0 & 0 & 0 & 0 \\ -\sigma & (\mu_H + \rho + \tau) & 0 & 0 & 0 \\ 0 & -\tau & (\mu_H + K_H + \omega) & 0 & 0 \\ 0 & 0 & 0 & (\phi_V + \mu_V) & 0 \\ 0 & 0 & 0 & -\phi_V & \mu_V \end{pmatrix}$$

$$J_V^{-1} = \begin{pmatrix} \frac{1}{(\sigma + \mu_H)} & 0 & 0 & 0 & 0 \\ \frac{\sigma}{((\sigma + \mu_H)(\mu_H + \rho + \tau))} & \frac{1}{(\mu_H + \rho + \tau)} & 0 & 0 & 0 \\ 0 & \frac{\tau}{(\mu_H + \rho + \tau)(\mu_H + K_H + \omega)} & \frac{1}{(\mu_H + K_H + \omega)} & 0 & 0 \\ 0 & 0 & 0 & \frac{1}{(\phi_V + \mu_V)} & 0 \\ 0 & 0 & 0 & \frac{\phi_V}{(\mu_V(\phi_V + \mu_V))} & \frac{1}{\mu_V} \end{pmatrix}$$

$$(3) \quad J_F J_V^{-1} = \begin{pmatrix} 0 & 0 & 0 & \frac{a\beta_1 \gamma \phi_V}{\mu_V (\mu_H + \alpha) (\phi_V + \mu_V)} & \frac{a\beta_1 \gamma}{\mu_V (\mu_H + \alpha)} \\ 0 & 0 & 0 & 0 & 0 \\ 0 & 0 & 0 & 0 & 0 \\ \frac{a\beta_2 \sigma \Lambda}{\mu_V (\mu_H + \rho + \tau) (\sigma + \mu_H)} & \frac{a\beta_2 \Lambda}{\mu_V} \left(\frac{(\mu_H + K_H + \omega) + \tau}{(\mu_H + \rho + \tau) (\mu_H + K_H + \omega)} \right) & \frac{a\beta_2 \Lambda}{(\mu_H + K_H + \omega) \mu_V} & 0 & 0 \\ 0 & 0 & 0 & 0 & 0 \end{pmatrix}$$

We obtain a non-zero sub-matrix A , which is a 2×2 block formed by the interaction between the non-zero entries of Eq. (3)

$$(4) \quad A = \begin{pmatrix} 0 & \frac{a\beta_1\gamma\phi_v}{\mu_v(\mu_H+\alpha)(\phi_v+\mu_v)} \\ \frac{a\beta_2\Lambda}{\mu_v} \left(\frac{(\mu_H+K_H+\omega)+\tau}{(\mu_H+\rho+\tau)(\mu_H+K_H+\omega)} \right) & 0 \end{pmatrix}$$

$$\lambda_{1,2}^* = \pm \sqrt{\left(\frac{a\beta_2\Lambda(\mu_H+K_H+\omega)+a\beta_2\Lambda\tau}{\mu_v(\mu_H+\rho+\tau)(\mu_H+K_H+\omega)} \right) \left(\frac{a\beta_1\gamma\phi_v}{\mu_v(\phi_v+\mu_v)(\mu_H+\alpha)} \right)}$$

Hence the largest eigenvalue gives

$$(5) \quad \mathfrak{R}_0 = \sqrt{\left(\frac{a\beta_2\Lambda(\mu_H+K_H+\omega)+a\beta_2\Lambda\tau}{\mu_v(\mu_H+\rho+\tau)(\mu_H+K_H+\omega)} \right) \left(\frac{a\beta_1\gamma\phi_v}{\mu_v(\phi_v+\mu_v)(\mu_H+\alpha)} \right)}$$

3.3. Local stability of \mathfrak{E}_0 .

The local stability of \mathfrak{E}_0 of system (2) is determined using the Next-Generation Matrix (NGM), such that \mathfrak{E}_0 is locally asymptotically stable whenever $\mathfrak{R}_0 < 1$ or otherwise.

$$J(\mathfrak{E}_0) = \begin{pmatrix} -k_1 & 0 & 0 & 0 & 0 & 0 & 0 & 0 & -\frac{a\beta_1\gamma}{\mu_H+\alpha} \\ 0 & -k_3 & 0 & 0 & 0 & 0 & 0 & 0 & 0 \\ 0 & \sigma & -k_4 & 0 & 0 & 0 & 0 & 0 & 0 \\ 0 & 0 & \tau & -k_5 & 0 & 0 & 0 & 0 & 0 \\ \alpha & 0 & 0 & 0 & -k_6 & 0 & 0 & 0 & 0 \\ 0 & 0 & \rho & \omega & \varepsilon & -\mu_H & 0 & 0 & 0 \\ 0 & 0 & -\frac{a\beta_2\Lambda}{\mu_v} & -\frac{a\beta_2\Lambda}{\mu_v} & 0 & 0 & -\mu_v & 0 & 0 \\ 0 & 0 & \frac{a\beta_2\Lambda}{\mu_v} & \frac{a\beta_2\Lambda}{\mu_v} & 0 & 0 & 0 & -k_8 & 0 \\ 0 & 0 & 0 & 0 & 0 & 0 & 0 & \phi_v & -\mu_v \end{pmatrix}$$

where the constants are defined as follows:

$$\begin{aligned} k_1 &= (\mu_H + \alpha), & k_2 &= a\beta_1\gamma, \\ k_3 &= (\sigma + \mu_H), & J &= (a\beta_1 I_V + \mu_H + \alpha), \\ k_4 &= (\mu_H + \rho + \tau), & k_5 &= (\mu_H + K_H + \omega), \\ k_6 &= (\varepsilon + \mu_H), & k_7 &= (\phi_v + \mu_v) \end{aligned}$$

The characteristic equation, given by $P(\lambda) = |\lambda I - J(E_0)| = 0$, is represented as:

$$P(\lambda) = \begin{vmatrix} \lambda + k_1 & 0 & 0 & 0 & 0 & 0 & 0 & 0 & -\frac{a\beta_1\gamma}{k_1} \\ 0 & \lambda + k_3 & 0 & 0 & 0 & 0 & 0 & 0 & 0 \\ 0 & \sigma & \lambda + k_4 & 0 & 0 & 0 & 0 & 0 & 0 \\ 0 & 0 & \tau & \lambda + k_5 & 0 & 0 & 0 & 0 & 0 \\ \alpha & 0 & 0 & 0 & \lambda + k_6 & 0 & 0 & 0 & 0 \\ 0 & 0 & \rho & \omega & \varepsilon & \lambda + \mu_H & 0 & 0 & 0 \\ 0 & 0 & -\frac{a\beta_2\Lambda}{\mu_V} & -\frac{a\beta_2\Lambda}{\mu_V} & 0 & 0 & \lambda + \mu_V & 0 & 0 \\ 0 & 0 & \frac{a\beta_2\Lambda}{\mu_V} & \frac{a\beta_2\Lambda}{\mu_V} & 0 & 0 & 0 & \lambda + k_7 & 0 \\ 0 & 0 & 0 & 0 & 0 & 0 & 0 & \phi_V & \lambda + \mu_V \end{vmatrix} = 0$$

According to the Gershgorin circle theorem [20], \mathfrak{E}_0 is locally asymptotically stable.

3.4. Global stability of \mathfrak{E}_0 .

We investigate the global stability of the disease-free equilibrium using the Castillo-Chavez theorem [21]. We express our model in the form:

$$(6) \quad \begin{cases} \frac{dX}{dt} = F(X, Y), \\ \frac{dY}{dt} = G(X, Y), \quad G(X, 0) = 0, \end{cases}$$

where $X = \{S_H, V_H, R_H, S_V\} \in \mathbb{R}^4$ represents the uninfected population, and $Y = \{E_H, I_H, D_H, E_V, I_V\} \in \mathbb{R}^5$ denotes the infected population. Let $E_0 = (X^*, 0)$, where

$$X^* = \left(\frac{\gamma}{\mu_H + \alpha}, 0, 0, 0, \frac{\alpha\gamma}{(\mu_H + \alpha)(\varepsilon + \mu_H)}, 0, \frac{\Lambda}{\mu_V}, 0, 0 \right).$$

The global asymptotic stability of E_0 , must satisfied the following:

- \mathfrak{H}_1 : If $\frac{dX}{dt} = F(X, 0)$, then X^* is said to be globally stable.
- \mathfrak{H}_2 : $\frac{dz}{dt} = D_Z G(X^*, 0) - \hat{G}(X, Z)$, with $\hat{G}(X, Z) \geq 0$ for all $(X, Z) \in \Omega$, where $D_Z G(X^*, 0)$ is the Jacobian of $G(X, Z)$ with regards to $(E_H, I_H, D_H, E_V, I_V)$.

If the system (2) satisfies the above conditions, then according to [21], the theorem below holds.

Theorem 2. *The equilibrium $E_0 = (X^*, 0)$ of system (2) is said to be globally asymptotically stable whenever $\mathfrak{R}_0 < 1$ such that \mathfrak{H}_1 and \mathfrak{H}_2 are fulfilled.*

Proof. From equation (6), $F(X, Y)$ and $G(X, Y)$ given as:

$$F(X, Y) = \begin{pmatrix} \gamma - \mu_H S_H - \alpha S_H \\ \alpha S_H - \varepsilon V_H - \mu_H V_H \\ \omega D_H + \rho I_H + \varepsilon V_H - \mu_H R_H \\ \Lambda - \lambda_2 - \mu_V S_V \end{pmatrix}, \quad G(X, Y) = \begin{pmatrix} \lambda_1 - (\sigma + \mu_H) E_H \\ \sigma E_H - (\mu_H + \rho + \tau) I_H \\ \tau I_H - (\mu_H + K_H) D_H - \omega D_H \\ \lambda_2 - (\phi_V + \mu_V) E_V \\ \phi_V E_V - \mu_V I_V \end{pmatrix}.$$

Now, from \mathfrak{H}_1 , the solution of $\frac{dX}{dt} = F(X, 0)$, as $t \rightarrow \infty$ is $X^* = \left(\frac{\gamma}{\mu_H + \alpha}, \frac{\alpha\gamma}{(\mu_H + \alpha)(\varepsilon + \mu_H)}, \frac{\Lambda}{\mu_V} \right)$.

Thus regardless of the initial condition, X^* is globally asymptotically stable.

The Jacobian $D_Z G(X^*, 0)$ is:

$$D_Z G(X^*, 0) = \begin{pmatrix} -k_3 & 0 & 0 & 0 & a\beta_1 S_H \\ \sigma & -k_4 & 0 & 0 & 0 \\ 0 & \tau & -k_5 & 0 & 0 \\ 0 & a\beta_2 S_V & a\beta_2 S_V & -k_7 & 0 \\ 0 & 0 & 0 & \phi_V & -\mu_V \end{pmatrix},$$

where, $k_3 = (\sigma + \mu_H)$, $k_4 = (\mu_H + \rho + \tau)$, $k_5 = (\mu_H + K_H + \omega)$, $k_7 = (\phi_V + \mu_V)$.

From condition H_2 , we compute:

$$\hat{G}(X, Z) = \begin{pmatrix} 0 \\ 0 \\ 0 \\ 0 \\ 0 \end{pmatrix}.$$

Since $\hat{G}(X, Z) \geq 0$, it is clear that the conditions \mathfrak{H}_1 and \mathfrak{H}_2 are satisfied and $E_0 = (X^*, 0)$ is global asymptotically stable. \square

3.5. Existence of endemic equilibrium point (\mathfrak{E}^*).

Given the transmission rates λ_H^{**} and λ_V^{**} , we define:

$$(7) \quad \begin{cases} \lambda_H^{**} = a\beta_1 I_V \\ \lambda_V^{**} = a\beta_2 (I_H + D_H) \end{cases}$$

The equilibrium states for the host and vector populations of system (2) are :

$$(8) \quad \left\{ \begin{array}{l} S_H^{**} = \frac{\gamma}{(\lambda_H^{**} + \mu_H + \alpha)} \quad E_H^{**} = \frac{\lambda_H^{**} S_H^{**}}{(\sigma + \mu_H)} \\ I_H^{**} = \frac{\sigma E_H^{**}}{(\mu_H + \rho + \tau)} \quad D_H^{**} = \frac{\tau I_H^{**}}{(\mu_H + K_H + \omega)} \\ V_H^{**} = \frac{\alpha S_H^{**}}{(\varepsilon + \mu_H)} \quad R_H^{**} = \frac{\omega D_H^{**} + \rho I_H^{**} + \varepsilon V_H^{**}}{\mu_H} \\ S_V^{**} = \frac{\Lambda}{(\lambda_2^{**} + \mu_V)} \quad E_V^{**} = \frac{\lambda_2^{**}}{(\phi_V + \mu_V)} \quad I_V^{**} = \frac{\phi_V E_V^{**}}{\mu_V} \end{array} \right.$$

3.6. Local Stability of \mathfrak{E}^* .

Theorem 3. *The point \mathfrak{E}^* of system (2) is locally asymptotically stable if $R_0 > 1$ and otherwise unstable.*

$$(9) \quad J(\mathfrak{E}^*) = \begin{bmatrix} -A & 0 & 0 & 0 & 0 & 0 & 0 & 0 & -a\beta_1 S_H^{**} \\ a\beta_1 I_V^{**} & -(\sigma + \mu_H) & 0 & 0 & 0 & 0 & 0 & 0 & 0 \\ 0 & \sigma & -k_4 & 0 & 0 & 0 & 0 & 0 & 0 \\ 0 & 0 & \tau & -k_5 & 0 & 0 & 0 & 0 & 0 \\ \alpha & 0 & 0 & 0 & -(\varepsilon + \mu_H) & 0 & 0 & 0 & 0 \\ 0 & 0 & \rho & \omega & \varepsilon & -\mu_H & 0 & 0 & 0 \\ 0 & 0 & -a\beta_2 S_V^{**} & -a\beta_2 S_V^{**} & 0 & 0 & -\mu_V & 0 & 0 \\ 0 & 0 & a\beta_2 S_V^{**} & a\beta_2 S_V^{**} & 0 & 0 & 0 & -(\phi_V + \mu_V) & 0 \\ 0 & 0 & 0 & 0 & 0 & 0 & 0 & \phi_V & -\mu_V \end{bmatrix}$$

where $A = (a\beta_1 I_V + k_1)$.

According to equation (9), $J(\mathfrak{E}^*)$ is a strictly column diagonally dominating matrix. Again, $(-A, -(\sigma + \mu_H) - k_4, -k_5, -(\varepsilon + \mu_H), -\mu_H, -(\phi_V + \mu_V), -\mu_V) < 0$, so all eigenvalues of $J(\mathfrak{E}^*)$ have a real part. Using the Gershgorin circle theorem [22], \mathfrak{E}^* is locally stable if

$$(10) \quad \left\{ \begin{array}{l} |A| > |a\beta_1 S_H|, \quad |\sigma + \mu_H| > |a\beta_1 I_V|, \quad |k_4| > |\sigma|, |k_5| > |\tau|, \\ \mu_V > |\phi_V| \quad |(\varepsilon + \mu_H)| > |\alpha|, \quad |\mu_H| > |\rho| + |\omega| + |\varepsilon|, \\ |\mu_V| > |a\beta_2 S_V| + |a\beta_2 S_V|, \quad |\phi_V + \mu_V| > |a\beta_2 S_V| + |a\beta_2 S_V|. \end{array} \right.$$

3.7. Global stability of \mathfrak{E}^* .

Theorem 4. *The endemic equilibrium \mathfrak{E}^* , of system (2) is globally asymptotically stable if $R_0 > 1$.*

Proof. Let L a Lyapunov function be defined by

$$\begin{aligned} L = & S_H^{**} \left(\frac{S_H}{S_H^{**}} - \ln \frac{S_H}{S_H^{**}} \right) + E_H^{**} \left(\frac{E_H}{E_H^{**}} - \ln \frac{E_H}{E_H^{**}} \right) + I_H^{**} \left(\frac{I_H}{I_H^{**}} - \ln \frac{I_H}{I_H^{**}} \right) \\ & + D_H^{**} \left(\frac{D_H}{D_H^{**}} - \ln \frac{D_H}{D_H^{**}} \right) + V_H^{**} \left(\frac{V_H}{V_H^{**}} - \ln \frac{V_H}{V_H^{**}} \right) + R_H^{**} \left(\frac{R_H}{R_H^{**}} - \ln \frac{R_H}{R_H^{**}} \right) \\ & + S_V^{**} \left(\frac{S_V}{S_V^{**}} - \ln \frac{S_V}{S_V^{**}} \right) + E_V^{**} \left(\frac{E_V}{E_V^{**}} - \ln \frac{E_V}{E_V^{**}} \right) + I_V^{**} \left(\frac{I_V}{I_V^{**}} - \ln \frac{I_V}{I_V^{**}} \right). \end{aligned}$$

By substituting model (2) into the derivative of L , we have

$$\begin{aligned} \dot{L} = & \left(1 - \frac{S_H^{**}}{S_H} \right) (\gamma - \lambda_1 S_H - \mu_H S_H - \alpha S_H) \\ & + \left(1 - \frac{E_H^{**}}{E_H} \right) (\lambda_1 S_H - (\sigma + \mu_H) E_H) + \left(1 - \frac{I_H^{**}}{I_H} \right) (\sigma E_H - (\mu_H + \rho + \tau) I_H) \\ & + \left(1 - \frac{D_H^{**}}{D_H} \right) (\tau I_H - (\mu_H + K_H + \omega) D_H) + \left(1 - \frac{V_H^{**}}{V_H} \right) (\alpha S_H - \varepsilon V_H - \mu_H V_H) \\ & + \left(1 - \frac{R_H^{**}}{R_H} \right) (\omega D_H + \rho I_H + \varepsilon V_H - \mu_H R_H) + \left(1 - \frac{S_V^{**}}{S_V} \right) (\Lambda - \lambda_2 S_V - \mu_V S_V) \\ & + \left(1 - \frac{E_V^{**}}{E_V} \right) (\lambda_2 S_V - (\phi_V + \mu_V) E_V) + \left(1 - \frac{I_V^{**}}{I_V} \right) (\phi_V E_V - \mu_V I_V). \end{aligned}$$

Collecting positive and negative terms together of the above leads to:

$$\frac{dL}{dt} = Q - K.$$

where

$$\begin{aligned} Q = & \alpha S_H + \lambda_1 S_H^{**} + \sigma E_H^{**} + \mu_H E_H^{**} + \mu_H I_H^{**} + \rho I_H^{**} + \tau I_H^{**} + \mu_H D_H^{**} \\ & + K_H D_H^{**} + \omega D_H + \varepsilon V_H^{**} + \lambda_2 S_V^{**} + \phi_V E_H^{**} + \mu_V E_H^{**} + \mu_V I_V + \mu_V I_V^{**}, \\ K = & \mu_H E_H + \lambda_1 S_H^{**} \frac{E_H^{**}}{E_H} + \mu_H I_H - \sigma I_H^{**} + \mu_H D_H + K_H D_H \\ & + \tau I_H \frac{D_H^{**}}{D_H} + \mu_H V_H + \alpha S_H \frac{V_H^{**}}{V_H} + \mu_H V_H^{**} + \mu_H R_H + \omega D_H \frac{R_H^{**}}{R_H} \\ & + \rho I_H \frac{R_H^{**}}{R_H} + \varepsilon V_H \frac{R_H^{**}}{R_H} + \mu_H R_H^{**} + \mu_V E_V + \lambda_2 S_V \frac{E_H^{**}}{E_H} + \phi_V I_V^{**} \frac{E_V^{**}}{I_V}. \end{aligned}$$

Thus, if $Q < K$, then $\frac{dI}{dt} \leq 0$. By LaSalle's invariant principle [23], \mathfrak{E}^* is globally asymptotically stable in Ω if $Q < K$. \square

4. SENSITIVITY ANALYSIS

To minimize the number of deaths and complications due to YF infections, it is vital to understand the relative relevance of several factors involved in the transmission and prevalence [24]. The forward sensitivity index of R_0 concerning the progression rate from infected to toxic infected class τ is given by:

$$\Pi_{\tau}^{R_0} = \frac{\partial R_0}{\partial \tau} \times \frac{\tau}{R_0} = -0.6264.$$

A similar approach when applied to the remaining parameters is shown in table 3. It can be observed that the mosquito biting rate, \mathbf{a} is the most significant parameter. This and other parameters have positive sensitivity indices while the remaining parameters in R_0 have negative indices.

TABLE 3. Sensitivity Indices of Parameters

Parameter	Sensitivity Index
a	1
β_1	0.5
σ	6.175×10^{-6}
γ	0.5
μ_H	-0.49999
K_H	-0.082793
Λ	0.5
α	-0.4975
β_2	0.5
ρ	-0.243986
τ	-0.6264
ϕ_V	0.000444

4.1. Numerical Simulation.

We perform a numerical simulation of the model (2) using parameter values in table 2 using Matlab ODE45 to ascertain its epidemiological implications. Figure 2a. shows how susceptible individuals decrease with time to 100 and become constant for the rest of the days.

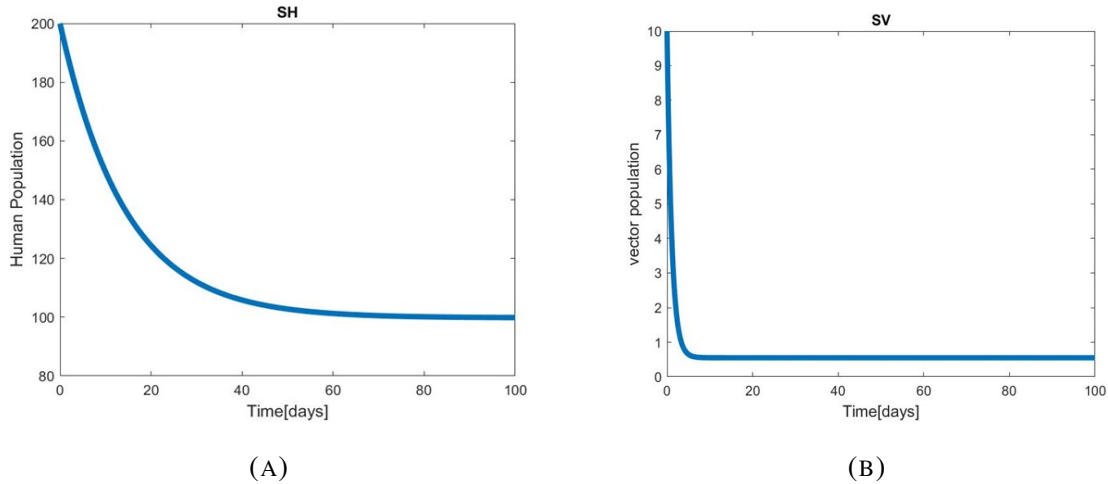


FIGURE 2. Simulation of susceptible humans S_H and host vectors S_V with time

The rapid decline in S_V is a result of the short life span of mosquitoes and more vectors moving into another compartment.

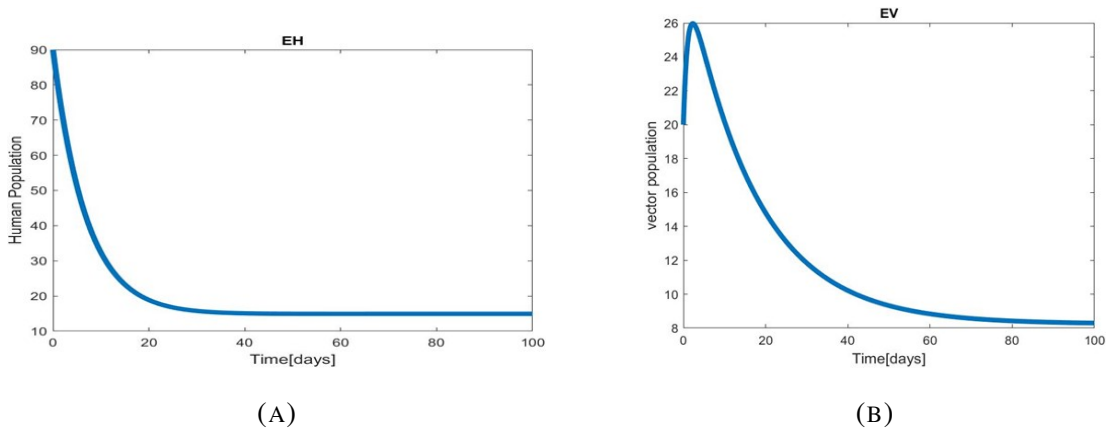


FIGURE 3. Simulation of exposed human and vectors over time

On the other hand, S_V with time declines from 10 to less than 1 within 10 days and remain constant for the rest of the time frame (Figure 2b). Figure 3a. displays how the exposed individuals with time decreases until it becomes constant after 30 days. The exposed vectors (Figure 3b.) rise from 20 and continue to move up until they get to their peak within the first 8 days and begin to decay with time. This is a result of more vectors getting infected.

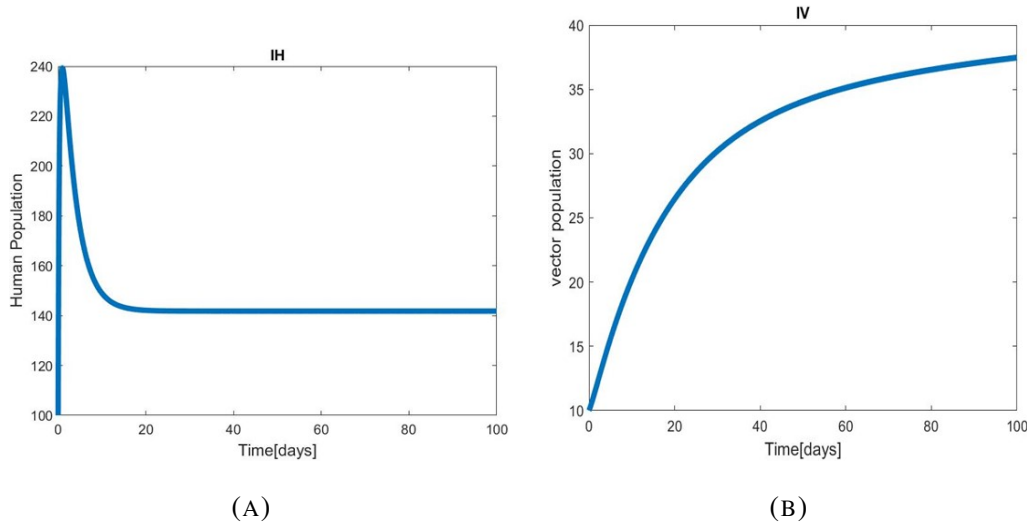


FIGURE 4. Simulation of infected human and vectors populations over time

The number of infected humans (Figure 4a.) increases rapidly at the initial state of the infections until it reaches its peak and then decreases with time before becoming constant after 10 days or more after the endemic. The increase in the infected vector at the initial stage indicates an initial outbreak phase followed by a stabilization period (Figure 4b). The infection rises sharply within the first 20 days, suggesting a high progression rate from E_V to I_V . After around 40 days, the curve starts to flatten, implying that the vector infection rate is slowing down. The stabilization suggests that either the number of E_V has reduced, or the mortality rate of vectors balances new infections. This highlights the importance of vector control measures in the early stages of an outbreak.

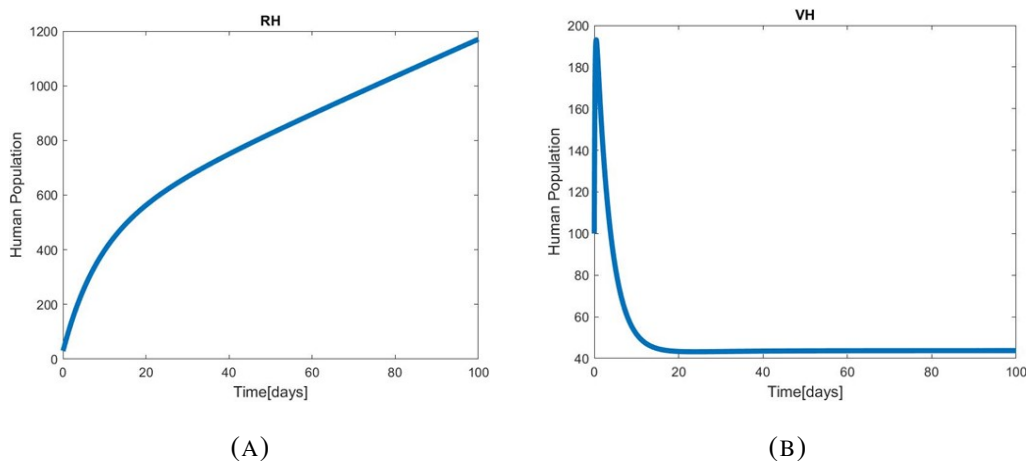


FIGURE 5. Simulation of recovered and vaccinated human population

Due to the increase in vaccination and treatment rates at different values, the recovered population increases steeply with time (Figure 5a), indicating that more people are being vaccinated against YF. Figure 5b, similar to the infected humans depicts the change in the vaccinated individuals with time. This demonstrates how the number of vaccinated individuals increases steadily within the first few days as infected people move into this compartment but later decreases when more people have taken the vaccine.

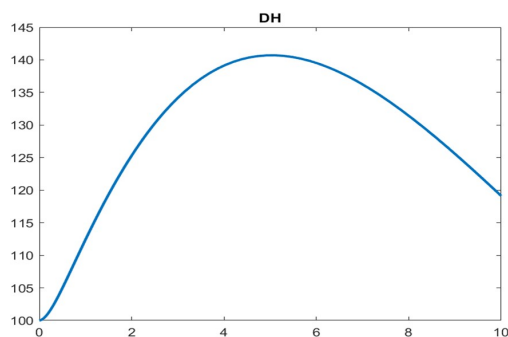


FIGURE 6. Simulation of toxic infected humans with time

Figure 6 illustrates how quickly infected individuals enter a toxic state, where the steep increase suggests a rapid progression from I_H to the toxic state due to high transmissibility. After 4 days, the toxic state reaches its peak, indicating the maximum burden of toxic infected cases. The gradual decrease is a result of increased recovery, reduced contact rates, or depletion of infectious individuals and possibly high mortality.

CONCLUSION

Transmission dynamics of yellow fever with a toxic infected population model were proposed and carefully analyzed within the perfect vaccinated population. The existence and stability analysis of the models' equilibrium points are investigated. Our sensitivity index analysis indicated $\mathbf{a}, \beta_1, \beta_2, \Lambda, \gamma$ were the most sensitive parameters influencing the spread of YF. The model is solved numerically using MATLAB ODE45 to ascertain its epidemiological implications. The increase in the infected vector at the initial stage is due to more susceptible vectors getting infected and becoming infectious (Figure 4b). Preventing progression from I_H to D_H is crucial, requiring timely treatment. Therefore to contain the spread, it is essential to reduce the contact rate of toxic individuals D_H with the susceptible population (S_H). The dynamics of D_H highlight the importance of focusing on severe cases to control outbreaks. Hence, interventions should aim to reduce the transition rate τ and increase recovery ω to mitigate the impact of toxic infections. Furthermore, the stabilization phase (figure 4b) implies that interventions targeting vector reproduction or mortality could help limit the spread of YF over time.

FUNDING

This research received no specific grant from funding agencies in the public, commercial, or not-for-profit sectors.

CONFLICT OF INTERESTS

The authors declare that there is no conflict of interests.

REFERENCES

- [1] J.-P. Chippaux, A. Chippaux, Yellow Fever in Africa and the Americas: A Historical and Epidemiological Perspective, *J. Venom. Anim. Toxins Incl. Trop. Dis.* 24 (2018), 20. <https://doi.org/10.1186/s40409-018-0162-y>.
- [2] J. Ye, B. Zhu, Z.F. Fu, H. Chen, S. Cao, Immune Evasion Strategies of Flaviviruses, *Vaccine* 31 (2013), 461–471. <https://doi.org/10.1016/j.vaccine.2012.11.015>.
- [3] S. Zhao, L. Stone, D. Gao, D. He, Modelling the Large-Scale Yellow Fever Outbreak in Luanda, Angola, and the Impact of Vaccination, *PLoS Negl. Trop. Dis.* 12 (2018), e0006158. <https://doi.org/10.1371/journal.pntd.0006158>.

- [4] A.A. Grobbelaar, J. Weyer, N. Moolla, P. Jansen Van Vuren, F. Moises, J.T. Paweska, Resurgence of Yellow Fever in Angola, 2015–2016, *Emerg. Infect. Dis.* 22 (2016), 1854–1855. <https://doi.org/10.3201/eid2210.160818>.
- [5] C. Possas, R. Lourenço-de-Oliveira, P.L. Tauil, et al. Yellow Fever Outbreak in Brazil: The Puzzle of Rapid Viral Spread and Challenges for Immunisation, *Mem. Inst. Oswaldo Cruz* 113 (2018), e180278. <https://doi.org/10.1590/0074-02760180278>.
- [6] T.T. Yusuf, D.O. Daniel, Mathematical Modeling of Yellow Fever Transmission Dynamics with Multiple Control Measures, *Asian Res. J. Math.* 13 (2019), 1–15. <https://doi.org/10.9734/arjom/2019/v13i430112>.
- [7] L.H. Chen, M.E. Wilson, Yellow Fever Control: Current Epidemiology and Vaccination Strategies, *Tropical Diseases, Travel Med. Vaccines* 6 (2020), 1. <https://doi.org/10.1186/s40794-020-0101-0>.
- [8] A.U. Nwaiwu, A. Musekiwa, J.L. Tamuzi, et al. The Incidence and Mortality of Yellow Fever in Africa: A Systematic Review and Meta-Analysis, *BMC Infect. Dis.* 21 (2021), 1089. <https://doi.org/10.1186/s12879-021-06728-x>.
- [9] F. Mushtaq, Z.A. Raza, S.R. Batool, et al. Preparation, Properties, and Applications of Gelatin-Based Hydrogels (GHs) in the Environmental, Technological, and Biomedical Sectors, *Int. J. Biol. Macromol.* 218 (2022), 601–633. <https://doi.org/10.1016/j.ijbiomac.2022.07.168>.
- [10] C. Baishya, S.J. Achar, D. Kumar, P. Veerasha, Dynamical Analysis of Fractional Yellow Fever Virus Model With Efficient Numerical Approach, *J. Comput. Anal. Appl.* 31 (2023), 140–157.
- [11] R.K. Mohapatra, S.L.V. Kutikuppala, A. Ansari, V. Kandi, S. Mishra, Another Neglected Tropical Disease Yellow Fever Re-Emerges in African Countries: Potential Threat in the COVID-19 Era Which Needs Comprehensive Investigations – Correspondence, *Int. J. Surg.* 108 (2022), 106988. <https://doi.org/10.1016/j.ijisu.2022.106988>.
- [12] S.D. Judson, E. Kenu, T. Fuller, et al. Yellow Fever in Ghana: Predicting Emergence and Ecology from Historical Outbreaks, *PLOS Global Public Health* 4 (2024), e0003337. <https://doi.org/10.1371/journal.pgph.0003337>.
- [13] N.L. Achee, J.P. Grieco, H. Vatandoost, et al. Alternative Strategies for Mosquito-Borne Arbovirus Control, *PLoS Negl. Trop. Dis.* 13 (2019), e0006822. <https://doi.org/10.1371/journal.pntd.0006822>.
- [14] F.B. Augusto, A.B. Gumel, P.E. Parham, Qualitative Assessment of the Role of Temperature Variations on Malaria Transmission Dynamics, *J. Biol. Syst.* 23 (2015), 1550030. <https://doi.org/10.1142/S0218339015500308>.
- [15] U. Danbaba, S. Garba, Stability Analysis and Optimal Control for Yellow Fever Model with Vertical Transmission, *Int. J. Appl. Comput. Math.* 6 (2020), 105. <https://doi.org/10.1007/s40819-020-00860-z>.
- [16] S. Martorano Raimundo, M. Amaku, E. Massad, Equilibrium Analysis of a Yellow Fever Dynamical Model with Vaccination, *Comput. Math. Methods Med.* 2015 (2015), 482091. <https://doi.org/10.1155/2015/482091>.

- [17] WHO, Situation Report: Yellow fever outbreak in Angola, 26 February 2016, World Health Organization. <https://www.afro.who.int/publications/situation-report-yellow-fever-outbreak-angola-26-february-2016>.
- [18] C.O. Onyango, V.O. Ofula, R.C. Sang, et al. Yellow Fever Outbreak, Imatong, Southern Sudan, *Emerg. Infect. Dis.* 10 (2004), 1064–1068. <https://doi.org/10.3201/eid1006.030738>.
- [19] D. Otoo, I.O. Abeasi, S. Osman, E.K. Donkoh, Mathematical modeling and analysis of the dynamics of hepatitis b with optimal control, *Commun. Math. Biol. Neurosci.* 2021 (2021), 43. <https://doi.org/10.28919/cmnb/5733>.
- [20] R.A. Horn, C.R. Johnson, *Matrix Analysis*, Cambridge University Press, 2012.
- [21] C. Castillo-Chavez, S. Blower, P. Van Den Driessche, D. Kirschner, A.-A. Yakubu, eds., *Mathematical Approaches for Emerging and Reemerging Infectious Diseases: Models, Methods, and Theory*, Springer New York, 2002. <https://doi.org/10.1007/978-1-4613-0065-6>.
- [22] D. Marquis, H. De Moor, K. Porter, M. Nathanson, Gershgorin’s Circle Theorem for Estimating the Eigenvalues of a Matrix with Known Error Bounds, Preprint, (2016).
- [23] J. Cao, Y. Wang, A. Alofi, et al. Global Stability of an Epidemic Model with Carrier State in Heterogeneous Networks, *IMA J. Appl. Math.* 80 (2015), 1025–1048. <https://doi.org/10.1093/imamat/hxu040>.
- [24] K.A. Gaythorpe, A. Hamlet, K. Jean, D. Garkauskas Ramos, L. Cibrelus, T. Garske, N. Ferguson, The Global Burden of Yellow Fever, *eLife* 10 (2021), e64670. <https://doi.org/10.7554/eLife.64670>.